

Lymphotoxin β receptor signaling is required for inflammatory lymphangiogenesis in the thyroid

Glucia C. Furtado*, Tatjana Marinkovic*, Andrea P. Martin*, Alexandre Garin*, Benjamin Hoch[†], Wolfgang Hubner[‡], Benjamin K. Chen*[‡], Eric Genden*[§], Mihaela Skobe*[¶], and Sergio A. Lira*[¶]

*Immunology Institute and Departments of [†]Pathology, [‡]Pharmacology and Biological Chemistry, [§]Otolaryngology, and [¶]Oncological Sciences, Mount Sinai School of Medicine, New York, NY 10029-6574

Edited by Nancy Ruddle, Yale University School of Medicine, New Haven, CT, and accepted by the Editorial Board January 22, 2007 (received for review August 3, 2006)

Infiltration of lymphocytes into the thyroid gland and formation of lymph node-like structures is a hallmark of Hashimoto's thyroiditis. Here we demonstrate that lymphatic vessels are present within these infiltrates. Mice overexpressing the chemokine CCL21 in the thyroid (TGCCCL21 mice) developed similar lymphoid infiltrates and lymphatic vessels. TGCCCL21 mice lacking mature T and B cells (RAGTGCCCL21 mice) did not have cellular infiltrates or increased number of lymphatic vessels compared with controls. Transfer of CD3⁺CD4⁺ T cells into RAGTGCCCL21 mice promoted the development of LYVE-1⁺podoplanin⁺Prox-1⁺ vessels in the thyroid. Genetic deletion of lymphotoxin β receptor or lymphotoxin α abrogated development of lymphatic vessels in the inflamed areas in the thyroid but did not affect development of neighboring lymphatics. These results define a model for the study of inflammatory lymphangiogenesis in the thyroid and implicate lymphotoxin β receptor signaling in this process.

chemokine | lymphatic vessels | CCL21

Lymphatic vessels have a pivotal role in homeostasis by controlling the transport of fluids and nutrients into circulation. In addition, lymphatic vessels have a critical role in the immune response because they are the main conduit for transport of antigen-presenting cells, memory and effector T cells, and soluble inflammatory mediators from peripheral tissues into the lymph nodes (1–4).

Lymphatic vessels develop during embryonic life by sprouting and lymphatic specialization of endothelial cells located on one side of embryonic cardinal veins (1). Lymphangiogenesis and remodeling of lymphatic vessels are not limited to embryogenesis; they occur throughout life during homeostasis and disease (1, 5, 6). Lymphangiogenesis has been described in wound healing; cancer; in many inflammatory conditions, including corneal inflammation, renal transplant rejection, chronic airway inflammation, Crohn's disease, and ulcerative colitis; and in the synovium of rheumatoid arthritis patients (7–12). *De novo* formation of lymphatic vessels during inflammation appears to involve macrophages, which are putative lymphatic progenitor cells and a source of lymphatic growth factors (7, 8, 13, 14). More recently, lymphangiogenesis has been described in the draining lymph nodes after immunization and was shown to depend on the entry of B cells into the node (15). Although the mechanisms leading to the development of lymphatic vasculature during embryonic development and tumorigenesis are relatively well understood, those affecting lymphangiogenesis in inflammatory conditions are not well characterized.

In particular, no information is available regarding the mechanisms responsible for the development of lymphatic vasculature found in tertiary lymphoid structures present in chronic inflammatory diseases, such as rheumatoid arthritis, Sjorgen's syndrome, diabetes mellitus, and autoimmune thyroiditis (16–20). Tertiary lymphoid structures are similar in organization to secondary lymphoid structures in that they have organized aggregates of T and B lymphocytes, dendritic cells, macrophages,

high endothelial venules (HEVs), and lymphatic vessels (20, 21). The formation of these tertiary lymphoid organs correlates with the expression of the chemokines CCL21, CCL19, and CXCL13 in humans (17, 20, 22). Expression of these chemokines in transgenic mice induce development of tertiary lymphoid structures very similar to those found in chronically inflamed tissues (23–26). These findings suggest that chemokines produced during inflammatory conditions may be sufficient to trigger tertiary lymph node organogenesis and HEV formation. To date, it is unclear whether chemokines are directly involved in the development of lymphatic vascular structures.

The best characterized factors for development of the embryonic lymphatic system, lymphatic regeneration in the adult, and tumor lymphangiogenesis are VEGF receptor 3 and its ligands VEGF-C and VEGF-D (2, 27). Other members of the VEGF family, such as VEGF-A and VEGFR-2, also have been implicated in lymphangiogenesis (28–30). In addition to VEGFs, several pleiotropic growth factors, such as basic FGF, hepatocyte growth factor, PDGF, and insulin-like growth factor can promote lymphangiogenesis under certain conditions (31). However, a role for these factors in *de novo* formation of lymphatic vessels in tertiary lymphoid structures has not been established.

Here we studied the formation of lymphatic vasculature within tertiary lymphoid tissue. We demonstrate that lymphatic vasculature is formed within tertiary lymphoid structures in the thyroid gland of patients with Hashimoto's thyroiditis. We also show that mature CD3⁺CD4⁺ T cells, recruited into the thyroid by transgenic expression of CCL21, can induce *de novo* lymphatic formation and that the lymphotoxin (LT) β receptor (LT β R)-signaling pathway is critical for this process. These findings directly implicate mature T cells, chemokines, and LT β R signaling in inflammatory lymphangiogenesis.

Results

Lymphatic Vessels Are Present Within Lymphoid Aggregates in Hashimoto's Thyroiditis. The formation of ectopic lymphoid structures is a hallmark of thyroid autoimmune diseases. To investigate whether lymphatic vessels were present within lymphoid aggregates, we examined thyroid specimens from four patients with Hashimoto's thyroiditis. In agreement with previous reports

Author contributions: G.C.F. and T.M. contributed equally to this work; G.C.F., T.M., E.G., M.S., and S.A.L. designed research; G.C.F., T.M., A.P.M., A.G., B.H., W.H., and M.S. performed research; G.C.F., T.M., A.P.M., A.G., B.K.C., and S.A.L. analyzed data; and G.C.F., T.M., M.S., and S.A.L. wrote the paper.

The authors declare no conflict of interest.

This article is a PNAS direct submission. N.R. is a guest editor invited by the Editorial Board.

Abbreviations: HEV, high endothelial venule; LEC, lymphatic endothelial cell; LT, lymphotoxin; LT β R, LT β receptor.

[¶]To whom correspondence should be addressed at: Immunology Institute, Mount Sinai School of Medicine, 1425 Madison Avenue, Box 1630, New York, NY 10029-6574. E-mail: sergio.lira@mssm.edu.

This article contains supporting information online at www.pnas.org/cgi/content/full/0606697104/DC1.

© 2007 by The National Academy of Sciences of the USA

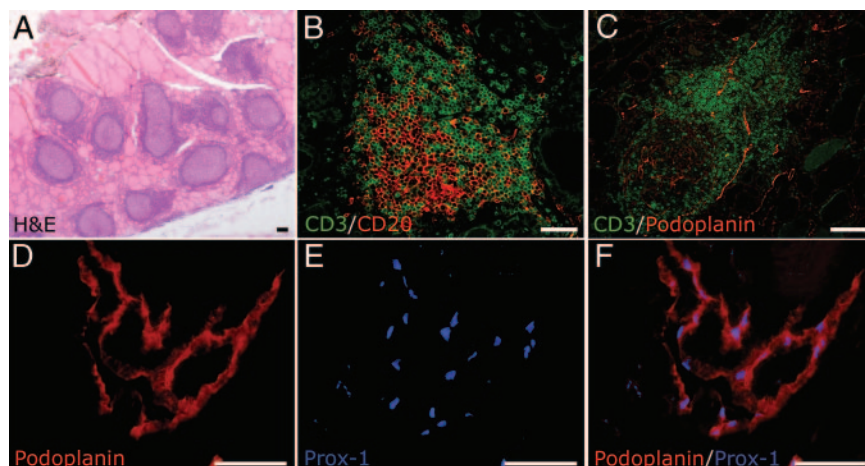


Fig. 1. Lymphatic vessels are present within lymphoid aggregates in Hashimoto's thyroiditis. (A) H&E-stained thyroid sections from patients with Hashimoto's thyroiditis showed the presence of the mononuclear cells aggregates. (B) Lymphocytic infiltration was visualized by using anti-CD3 and anti-CD20 antibodies. (C) Podoplanin-positive lymphatic vessels were present within lymphocytic infiltrates (visualized by CD3 staining) in the thyroids of all cases studied ($n = 4$). (D and E) Higher magnification of lymphatic vessels stained with podoplanin (D) and Prox-1 (E) antibodies. (F) Colocalization of podoplanin and Prox-1 in lymphatic vessels. (Scale bars, 25 μm .)

(32), we detected lymphoid aggregates containing T and B cells (Fig. 1A and B). Lymphatic vessels, stained with antibodies for LYVE-1 (data not shown), podoplanin, and Prox-1 (33, 34) were prominent in all Hashimoto's thyroiditis specimens analyzed (Fig. 1C–F). Lymphatic vessels were found in the periphery and in the midst of lymphocytic infiltrates (Fig. 1C). These vessels were more abundant in the areas containing aggregates than in the noninfiltrated areas (data not shown). The presence of specialized lymphatic vasculature within the lymphoid aggregates suggested an association between lymphocyte accumulation and lymphangiogenesis.

Lymphatic Vessels Are Present Within Lymphoid Aggregates Induced by the Expression of CCL21 in the Thyroid of Transgenic Mice. To study the mechanisms associated with development of lymphatic vessels within lymphoid aggregates, we used the TGCCCL21 trans-

genic model, in which the chemokine CCL21 is overexpressed in the thyroid (24). This model mimics two key aspects of Hashimoto's thyroiditis: the ectopic expression of CCL21 in the thyroid (22) and the formation of intrathyroidal lymphoid follicles characterized by segregated T and B cell zones and formation of PNA⁺ HEVs (24).

To investigate the presence of lymphatic vessels within the thyroid we used an anti-LYVE-1 antibody (35). LYVE-1⁺ cells were mostly found around the thyroid and occasionally within the thyroid parenchyma of control mice (Fig. 2A). In marked contrast, large LYVE-1-positive vessels were found in the midst of lymphocytic infiltrates of the thyroids of TGCCCL21 mice (Fig. 2B and C). To confirm that these LYVE-1⁺ cells were lymphatic endothelial cells, we examined the expression of the panendothelial marker CD31. LYVE-1⁺ cells represented a subset of CD31⁺ cells (Fig. 2D). Similar to lymphatic endothelial cells

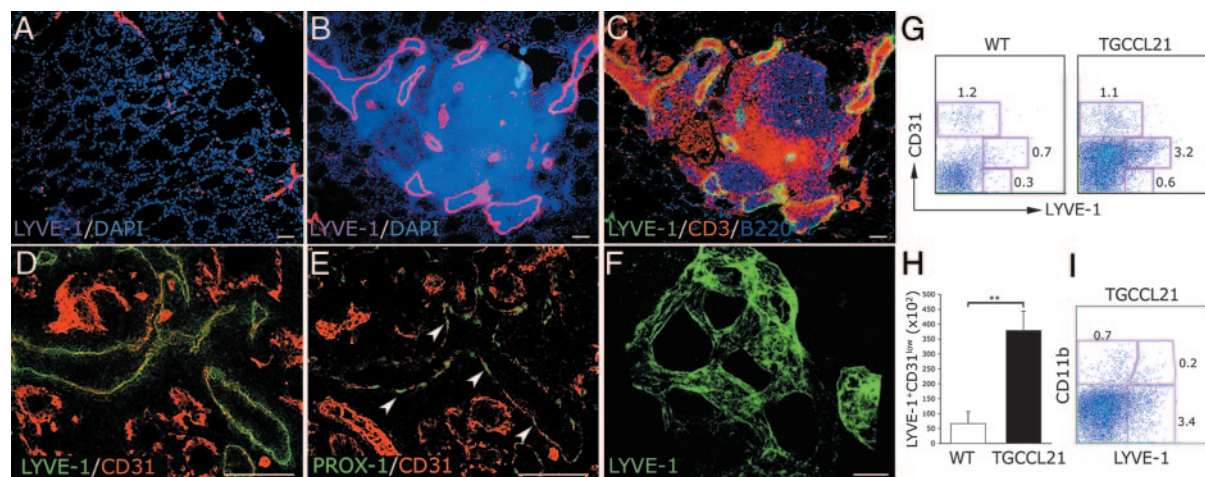


Fig. 2. Lymphatic vessels are present within lymphoid aggregates in the thyroids of TGCCCL21 mice. (A and B) Thyroids from wild-type (A) and TGCCCL21 (B) mice were examined for the presence of lymphatic vessels. (B) LYVE-1⁺ vessels (magenta) were abundant in infiltrated areas of TGCCCL21 thyroid (revealed by DAPI counterstain). (C) LYVE-1⁺ vessels (green) were present within both T cell (CD3, red) and B cell (B220, blue) areas. (D and E) LYVE-1⁺ vessels present in the thyroid of TGCCCL21 mice ($n = 6$) also were positive for the endothelial marker CD31 (D) and lymphatic marker Prox-1 (arrowheads point to PROX-1⁺ nuclei) (E). (F) Confocal analysis of the whole-mount thyroid revealed the presence of a complex lymphatic network in the thyroid of TGCCCL21 mice. (G–I) Flow-cytometric analysis revealed increased relative and absolute numbers of LYVE-1⁺CD31^{low} cells in the thyroid of TGCCCL21 mice. Data are mean \pm SEM ($n = 4$ mice; **, $P < 0.01$). (Scale bars, 25 μm .)

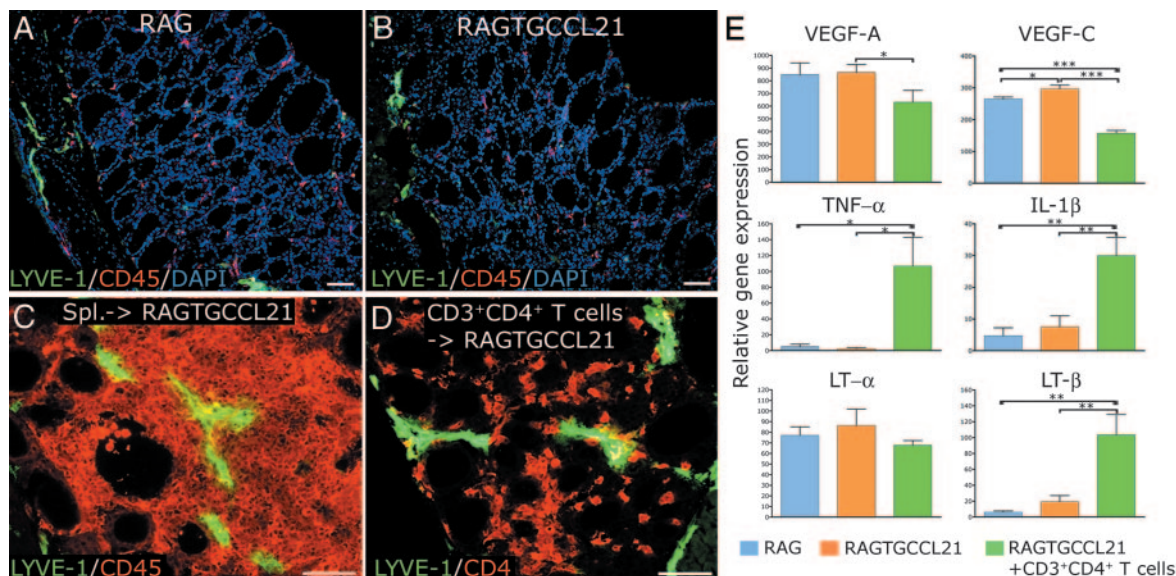


Fig. 3. CD3⁺CD4⁺ T cells induce formation of lymphatic vessels in the thyroid. (A and B) Thyroids from RAG (A) and RAGTGCCL21 (B) mice were stained with anti-LYVE-1, anti-CD45 antibodies, and DAPI (blue). No obvious differences were observed between the two strains ($n = 3$ per group). (C) Splenocytes (10^7) were injected i.v. into RAGTGCCL21 mice. Large numbers of CD45⁺ cells and LYVE-1⁺ vessels were observed in the thyroids 2 months after transfer ($n = 3$). (D) Purified CD3⁺CD4⁺ T cells (10^6) were injected into RAGTGCCL21 mice. Ten days after transfer, LYVE-1⁺ vessels were detected in the thyroids of all RAGTGCCL21 mice examined ($n = 5$). (Scale bars, 100 μ m.) (E) Relative levels of mRNA for the indicated genes in the thyroids of RAG, RAGTGCCL21, and RAGTGCCL21 mice injected with 10^6 CD3⁺CD4⁺ T cells for 10 days were determined by quantitative PCR. Results are mean \pm SEM. Three animals of each genotype were used in these experiments (*, $P < 0.05$; **, $P < 0.01$; ***, $P < 0.001$).

(36), this subset expressed low levels of CD31 (Fig. 2D). Analysis of adjacent sections showed that the LYVE-1⁺CD31⁺ vessels expressed Prox-1 (Fig. 2E), a key transcription factor for the differentiation of lymphatic endothelial cells (34, 37). Finally, confocal analysis of whole-mount thyroids revealed that the LYVE-1⁺ vessels located in the center of the infiltrates were connected to the vessels at the periphery, forming a complex network (Fig. 2F) similar to the lymphatic network found in other organs.

Next, we performed flow cytometry to quantify and further characterize the lymphatic vessels found in the thyroid of TGCCL21 mice. We observed a 3- to 4-fold increase in the relative and absolute numbers of LYVE-1⁺CD31^{low} cells in the thyroids of transgenic mice compared with controls (Fig. 2G and H). To differentiate LYVE-1⁺ endothelial cells from macrophages, which also express LYVE-1 (8, 14), we used an anti-CD11b antibody. We found that most LYVE-1⁺ cells in the thyroid of TGCCL21 mice did not stain with an anti-CD11b antibody (Fig. 2I). Together, these results indicate that expression of CCL21 in the thyroid induced the development of organized lymphoid aggregates and bona fide lymphatic vasculature.

Purified CD4⁺ T Cells Induce Formation of Lymphatic Vessels in the Thyroid. To determine whether the development of lymphatic vessels in the thyroid of TGCCL21 mice was attributable to a direct effect of CCL21 on endothelial cells, we crossed TGCCL21 mice with RAG mice to obtain animals that expressed CCL21 in the thyroid and lacked T and B cells (RAGTGCCL21 mice). There were no significant differences in the number or localization of LYVE-1⁺ vessels in the thyroids of RAG and RAGTGCCL21 mice (Fig. 3A and B), indicating that the chemokine CCL21 was not sufficient to trigger lymphangiogenesis in the absence of T and B cells.

To investigate whether the infiltrating lymphocytes were responsible for the CCL21-triggered induction of lymphangiogenesis in the thyroid, we performed adoptive transfer of splenocytes into RAGTGCCL21 mice. As we previously described

(24), adoptively transferred splenocytes accumulated in the thyroid of RAGTGCCL21 mice. More important, the accumulation of splenocytes in the thyroid was accompanied by the formation of LYVE-1⁺ vessels in the midst of the infiltrates (Fig. 3C). To determine which cell type triggered development of lymphatics, we sorted distinct cell populations from the spleen, adoptively transferred them to RAGTGCCL21 mice, and examined their thyroids 10 days later. Adoptive transfer of highly purified CD3⁺CD4⁺ T cells led to accumulation of lymphocytes and myeloid cells of host origin in the thyroid of RAGTGCCL21 but not RAG mice (Fig. 3D) (38). Purified CD8⁺ T cells or B cells did not accumulate in the thyroid of RAGTGCCL21 mice (data not shown). Within these aggregates, LYVE-1⁺ cells could be readily identified (Fig. 3D). These findings indicated that the influx of CD3⁺CD4⁺ T cells triggered lymphangiogenesis in the thyroid.

To characterize the factors that facilitated development of lymphatic vessels in the thyroid, we extracted mRNA from the thyroids of RAG, RAGTGCCL21, and RAGTGCCL21 mice that had received CD3⁺CD4⁺ T cells and compared the expression levels of several cytokines implicated in inflammation, angiogenesis, and lymphangiogenesis (Fig. 3E). Surprisingly, the expression of mRNA for VEGF-C, one of the most important factors for lymphangiogenesis and VEGF-A, a key angiogenic molecule (1), was reduced on influx of CD3⁺CD4⁺ cells (Fig. 3E). There were no changes in the levels of mRNA for other lymphangiogenic factors such as insulin-like growth factor-1 and -2 and their receptors (data not shown) (39). Interestingly, the infiltration of CD3⁺CD4⁺ T cells in the thyroid induced expression of the proinflammatory cytokines TNF α and IL-1 β , and up-regulated LT β (Fig. 3E). Together, these results suggested that the process of *de novo* lymphangiogenesis in the thyroid was induced by infiltrating cells and that it did not require overexpression of classical lymphatic growth factors.

Lymphangiogenesis in the Thyroid Depends on LT β R Signaling. The importance of LT β and its receptor LT β R for the development of

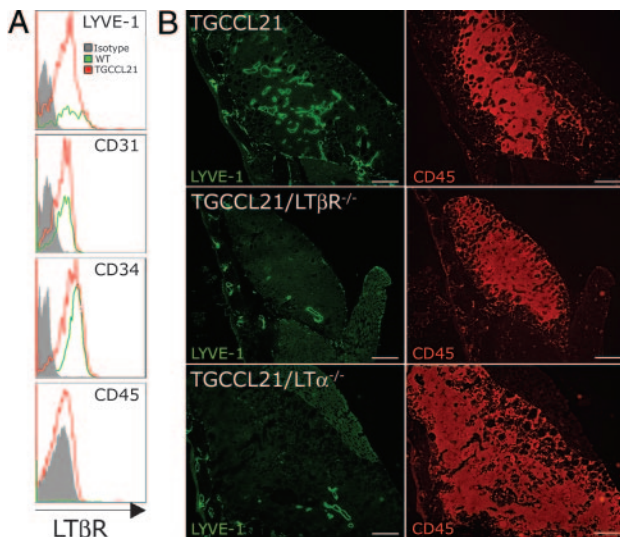


Fig. 4. $LT\beta R$ and $LT\alpha$ deficiency impairs formation of lymphatic vessels in the thyroid. (A) Flow-cytometric analysis of $LT\beta R$ expression in LYVE-1, CD31, CD34, and CD45 cell subsets present in the thyroid of wild-type ($n = 7$) and TGCCCL21 mice. The isotype control is represented by the gray tracing. Representative results of two independent experiments are shown. (B) Thyroids from TGCCCL21, TGCCCL21/ $LT\beta R^{-/-}$, and TGCCCL21/ $LT\alpha^{-/-}$ mice were stained with anti-LYVE-1 and CD45 antibodies. Compared with TGCCCL21 mice ($n = 3$), the number and size of LYVE-1⁺ vessels were significantly reduced in both TGCCCL21/ $LT\beta R^{-/-}$ ($n = 7$) and TGCCCL21/ $LT\alpha^{-/-}$ ($n = 3$) mice. Representative staining is shown. (Scale bars, 250 μm .)

secondary lymphoid organs and PNA⁺ HEV is well documented (40–43), but the mechanisms that govern formation of the lymphatic vasculature are still poorly understood. Our finding that entry of CD3⁺CD4⁺ T cells in the thyroid promoted lymphangiogenesis and induced $LT\beta$ expression prompted us to investigate the contribution of $LT\beta R$ signaling to lymphangiogenesis.

We examined the distribution of $LT\beta R$ -positive cells within the thyroids of wild-type and TGCCCL21 mice by flow cytometry. In both wild-type and TGCCCL21 mice, $LT\beta R$ expression was found on cells expressing the endothelial markers CD31 and CD34 (Fig. 4A). Importantly, the majority of the LYVE-1⁺ cells expressed $LT\beta R$ (Fig. 4A). As expected, the number of $LT\beta R$ -positive cells within the thyroid increased with the lymphocytic infiltration. This finding reflected an increase in the number of LYVE-1⁺ cells rather than an increase in the CD45⁺ cells because $LT\beta R$ was not significantly expressed on CD45⁺ cells (Fig. 4A). Immunostaining of TGCCCL21 thyroids with anti- $LT\beta R$ antibodies showed colocalization of $LT\beta R$ with CD31⁺ vessels, LYVE-1⁺ lymphatic cells, and PNA⁺ HEVs [supporting information (SI) Fig. 5], in agreement with previous results (47). Expression of $LT\beta R$ also was detected in human lymphatic endothelial cells (LECs) by quantitative PCR (36) (SI Fig. 6A).

To investigate the importance of $LT\beta R$ signaling in *de novo* lymphangiogenesis, we crossed TGCCCL21 mice with $LT\beta R$ -deficient animals (40) and examined the thyroids of the resulting mice for lymphocytic infiltration and lymphatic vessels. CD45⁺ cells accumulated in the thyroid in the absence of $LT\beta R$, but the number of lymphatic vessels was significantly reduced in the thyroids of TGCCCL21/ $LT\beta R^{-/-}$ mice compared with TGCCCL21/ $LT\beta R^{+/+}$ littermates (Fig. 4B). Of note, $LT\beta R$ deficiency specifically affected *de novo* lymphangiogenesis in areas with lymphocytic infiltrates; lymphatic vessels were readily identified in the adjacent normal tissue of both strains.

To determine which $LT\beta R$ ligand mediated lymphangiogenesis in the thyroid, we crossed TGCCCL21 mice with the animals deficient for $LT\alpha$ (44). These animals lacked both $LT\alpha$ and the

$LT\beta R$ ligand $LT\alpha 1\beta 2$ (45). Similar to what was observed with TGCCCL21/ $LT\beta R^{-/-}$ mice, $LT\alpha$ deficiency did not affect influx of CD45⁺ cells in the thyroids of TGCCCL21 mice (Fig. 4B). However, the lymphatic vessels in the thyroid of TGCCCL21/ $LT\alpha^{-/-}$ mice were reduced in number and size (Fig. 4B), suggesting that $LT\alpha$ is required for growth of lymphatic vessels during formation of tertiary lymphoid structures. To examine how $LT\beta R$ signaling affected appearance of the lymphatic vasculature, we performed *in vitro* studies. $LT\beta R$ was abundantly expressed by LECs and TNF α treatment further increased $LT\beta R$ expression, as demonstrated by quantitative PCR (SI Fig. 6). To examine the effects of $LT\beta R$ signaling on cell proliferation, we treated LECs with various concentrations of $LT\alpha 1\beta 2$ (0–100 ng/ml) and analyzed cell proliferation 48 h later. We did not observe any effect of $LT\alpha 1\beta 2$ on LEC proliferation even after 72 h of cell culture. In contrast, $LT\alpha 1\beta 2$ treatment promoted LEC tube formation in a collagen gel. These results indicate that $LT\alpha 1\beta 2$ exerts a direct effect on the tubular organization of LECs *in vitro*. Together, these findings indicate that $LT\beta R$ signaling is involved in lymphangiogenesis associated with the formation of tertiary lymphoid structures.

Discussion

In this study we show that lymphatic vessels are present within the lymphoid infiltrates commonly found in the thyroids of patients with Hashimoto's thyroiditis and present evidence that *de novo* lymphangiogenesis in the thyroid depends on CCL21, mature T cells, and $LT\beta R$ signaling.

By using a transgenic mouse model, we demonstrate that the process of tertiary lymphoid organogenesis involves generation of lymphatic vessels. This process can be induced by recruitment of T cells into areas overexpressing the chemokine CCL21. Expression of CCL21 is commonly detected in lymphoid aggregates found in many inflammatory conditions, including Hashimoto's thyroiditis (20, 22). The transgenic model used in this study reproduces key aspects of the human disease, including chemokine expression, distinctly arranged T and B cell areas, and development of specialized vascular structures including HEVs and lymphatics (this study and ref. 24). The expression of CCL21, however, was not sufficient to trigger lymphangiogenesis. The density of lymphatics in the thyroid of RAG mice that expressed CCL21 in the thyroid was similar to that of RAG mice.

We show here that transfer of purified CD3⁺CD4⁺T cells into B cell-deficient RAGTGCCCL21 mice induces lymphangiogenesis in the thyroid. Recent work by Angeli *et al.* (15) indicates a requirement for B cells for lymphangiogenesis in inflamed lymph nodes. Although B cells are required for the expansion of already existing lymphatic vessels in the lymph nodes, they seem to be dispensable for *de novo* formation of lymphatic vessels in our model. At this point, it is unclear how CD3⁺CD4⁺ T induce lymphangiogenesis. They may act directly to modify the lymphatic vasculature, or indirectly, via production of lymphatic growth factors, cytokines, and chemokines. We have recently shown that transfer of T cells is associated with changes in the expression of chemokines and with influx of host-derived dendritic cells (38). Thus, it is possible that other cells, such as host-derived dendritic cells or other myeloid cells, may be involved in lymphangiogenesis in this model.

The lymphatic vessels present in the thyroids of TGCCCL21 mice may have been formed by sprouting from the preexisting lymphatic vessels or from lymphatic progenitors recruited into the thyroid. Circulating bone marrow-derived VEGF receptor-3⁺CD34⁺CD133⁺ cells and macrophages have been identified as the precursors of lymphatic endothelial cells (8, 14, 46). Further study is necessary to define whether the lymphatic vessels in the thyroid of TGCCCL21 mice are formed by the recruitment of progenitor cells in the thyroid.

Which molecules mediate lymphangiogenesis induced by influx of CD3⁺CD4⁺ T cells in the thyroid? Our results indicate that the effects of CCL21 and those brought about by the infiltrating cells do not involve substantial changes in the transcription of VEGF genes involved in lymphangiogenesis. The levels of mRNA for VEGF-C and VEGF-A were reduced rather than increased upon entry of CD3⁺CD4⁺ T cells in the thyroid. Furthermore, treatment of animals adoptively transferred with T cells with a VEGF receptor-3 blocking antibody did not inhibit formation of lymphatic vessels (G.C.F., M.S., and S.A.L., unpublished results). These results suggest that *de novo* formation of lymphatic vessels in this model does not require overexpression of VEGFs by infiltrating cells. However, these findings do not exclude the possibility that VEGFs contribute to some aspect of lymphatic vessel formation or stabilization.

The influx of T cells in the thyroid resulted in marked changes in the expression of the proinflammatory mediators TNF α and IL-1 β , confirming the inflammatory nature of the process. We hypothesize that these cytokines may contribute to lymphangiogenesis by facilitating the expression or processing of lymphatic endothelial growth factors and/or recruitment of lymphatic progenitor cells.

Among the changes promoted by the influx of CD3⁺CD4⁺ T cells into the thyroid was the up-regulation of LT β expression. Further investigation revealed that the LT/LT β R system was required for the formation of lymphatics in the thyroid. LT β R signaling is important for the formation and maintenance of the HEVs in lymph nodes (41, 47–49), but until now, a link between LT β R and the formation of lymphatic vessels in tertiary lymphoid tissue has not been established. We demonstrate here that endothelial cells in the thyroid constitutively expressed LT β R and that deficiency of both LT β R and its ligand LT α 1 β 2 reduced the number and the size of lymphatic vessels present in the tertiary lymphoid structure in the thyroid but did not affect the number of lymphatic vessels in the neighboring tissue. These results suggest that LT β R signaling is not required for embryonic development of lymphatic vessels but that it is necessary for *de novo* formation of lymphatic vessels associated with inflammation. We propose that LT β R ligands, expressed by infiltrating cells, trigger the development of the lymphatic vasculature within the aggregates.

For years, the lymphatic system has been considered primarily a drainage system for interstitial fluid and macromolecules. Only recently the importance of lymphatic vessels for the function of immune system has been appreciated. The finding that LT β R is required for pathological lymphangiogenesis but not for the formation and maintenance of lymphatic vessels in noninflamed tissue suggests the existence of specialized developmental programs for the formation of lymphatic vessels with primary immune function. Whether there are functional differences between these lymphatic vessels remains to be evaluated.

In conclusion, we show that lymphangiogenesis is a hallmark of tertiary lymphoid organogenesis and that its minimal requirements include expression of CCL21, recruitment of CD3⁺CD4⁺T cells, and LT β R signaling. As the formation of a lymphatic vascular supply may constitute a pathway for trafficking of lymphoid and dendritic cells within the aggregates, it will be important to define whether interference with the LT β R system and lymphatic development will affect chronic inflammatory diseases.

Materials and Methods

Human Tissue. Human thyroid tissue was obtained as part of routine patient care and diagnostic pathological examination at the Mount Sinai Medical Center. The diagnosis of Hashimoto's thyroiditis was confirmed by microscopic examination of the routine H&E-stained slides by using established histopathologic criteria, including lymphocytic and plasmacytic infiltration of the

gland with formation of lymphoid follicles and occasional HEVs, infiltration and destruction of thyroid follicles by lymphocytes, and variable amounts of fibrosis and oncocytic (Hürthle cell) cytological changes. Normal thyroid tissue was used as a control.

Mice. Mice expressing CCL21 under the control of the thyroglobulin promoter (TGCCL21 mice) have been described (24). TGCCL21 mice were crossed to RAG2^{-/-} mice (50) (The Jackson Laboratory, Bar Harbor, ME) to obtain animals that specifically overexpress CCL21 in the thyroid and lack T and B cells (RAGTGCCL21). LT β R^{-/-} and LT α ^{-/-} mice (40, 44) were crossed to TGCCL21 mice to obtain TGCCL21/LT β R^{-/-} and TGCCL21/LT α ^{-/-} mice, respectively.

All mice were housed under specific, pathogen-free conditions in individually ventilated cages at the Mount Sinai School of Medicine Animal Facility. All experiments were performed according to institutional guidelines.

Histology. For examination of human thyroids, 3- μ m sections were cut from paraffin-embedded tissue from the cases of Hashimoto's thyroiditis, deparaffinized, and treated with citrate-based antigen retrieval solution (DAKO, Carpinteria, CA). Mouse tissue samples were embedded in OCT buffer (Sakura Finetek, Torrance, CA), snap-frozen, cryosectioned (8- μ m thick), and fixed in acetone. Sections were blocked and incubated with primary antibodies in a humidified atmosphere for 1 h at room temperature. After washing, conjugated secondary antibodies were added for 35 min. The slides were then washed and mounted with Fluoromount-G (Southern Biotech, Birmingham, AL).

Antibodies used for staining of human tissue were specific for CD3 and CD20 (DAKO), podoplanin (Serotec, Raleigh, NC), and Prox-1 (Upstate, Lake Placid, NY). Mouse tissues were stained with antibodies against LYVE-1, Prox-1 (both from Upstate), LT β R (R & D Systems, Minneapolis, MN), CD31, CD3, CD4, CD45, and B220 (PharMingen, San Diego, CA). The secondary antibodies used were Alexa Fluor 594 anti-rat IgG; Alexa Fluor 488 anti-rat IgG and anti-rabbit IgG from Molecular Probes (Eugene, OR); and Cy3 anti-Armenian hamster, Cy5 anti-rat (Jackson ImmunoResearch, West Grove, PA). In some instances, slides were counterstained with DAPI (Fluka, Buchs, Switzerland). Analysis was performed by using a Nikon (Tokyo, Japan) Eclipse E-600 fluorescence microscope and Photoshop software (Adobe Systems, Mountain View, CA). To improve visualization, the original color obtained with Alexa Fluor 488 was changed to red (Fig. 2A and B), and the color obtained with Cy5 was changed to blue (Fig. 2C). For the confocal analysis, 100- μ m thick thyroid sections were stained with anti-LYVE-1 and anti-CD45 antibodies.

For the analysis of the lymphatic network, whole-thyroid lobes were carefully detached from surrounding tissue, fixed in acetone, and stained with anti-LYVE-1 antibody. Images were obtained by using an LSM 510 META confocal fluorescence microscope (Zeiss, Jena, Germany) and analyzed with ImageJ (<http://rsb.info.nih.gov/ij/>) and Volocity software packages (Improvision, Coventry, U.K.).

Flow Cytometry. To obtain single-cell suspensions, thyroids were incubated in RPMI medium 1640 containing 0.25 mg/ml Liberase Blendzyme 3 (Roche Applied Science, Indianapolis, IN) at 37°C for 30 min and then passed through a 100- μ m nylon cell strainer (BD Discovery Labware, Bedford, MA). Cells were stained for 40 min on ice and analyzed in a FACSCanto cytometer (Becton Dickinson, Franklin Lakes, NJ). LYVE-1⁺ cells were detected by using rabbit anti-LYVE-1 antibody (Upstate) followed by conjugated anti-rabbit secondary antibody. For detection of CD11b, CD31, CD34, and CD45, directly conjugated antibodies were used (PharMingen). LT β R expression was detected by using biotinylated specific antibody (R & D

Systems) and revealed by using fluorochrome-conjugated streptavidin (PharMingen).

Cell Purification and Transfer. Single-cell suspensions were prepared by passing spleen tissue through a nylon mesh. Splenocytes (1×10^7) were resuspended in 100 μ l of PBS and injected into the retroorbital sinus. For the transfers of CD4⁺ T cells, splenocytes were labeled by using directly conjugated CD4 and CD3 antibodies (PharMingen) and sorted by using a MoFLOW cell sorter (Dako-Cytomation, Ft. Collins, CO) according to standard protocols. The purity of the sorted populations was >98%. For transfers, purified cells (1×10^6) were resuspended in 100 μ l of PBS and injected into the retroorbital sinus. Mice were killed at the time points indicated in Fig. 3, and thyroids were removed and analyzed by immunohistochemistry.

Analysis of mRNA Expression. Total RNA was extracted from the thyroid by using an RNeasy mini kit (Qiagen, Valencia, CA) according to the instructions of the manufacturer. Reverse transcription was performed by using 2 μ g of total RNA. Quantitative PCR was conducted in duplicates by using 25 ng of reverse-transcribed cDNA and each primer at 0.4 μ M in a 30- μ l

final reaction volume containing 1 \times SYBR Green PCR Master Mix (Applied Biosystems, Foster City, CA). PCR-cycling conditions were as follows: 50°C for 2 min; 95°C for 10 min and 40 cycles of 95°C for 15 sec; and 60°C for 1 min. Relative expression levels were calculated as $2^{-(\text{threshold cycle [Ct]} \text{ubiquitin} - \text{Ct gene})}$, where Ct indicates cycle threshold (for details, see User Bulletin No. 2, ABI PRISM 7700; Applied Biosystems), by using ubiquitin RNA as an endogenous control. We used a two-tailed Student *t* test to evaluate statistically significant differences in expression levels of specific chemokines. Primers were designed by using Primer Express 2.0 software (Applied Biosystems). Primer sequences are described in SI Table 1.

We thank Claudia Canasto-Chibuque, Sabine Mofina, and Bryan Kloos for expert technical assistance with the mouse colony, *in situ* hybridization, and tube formation assays, respectively; Jay Unkeless, Terry Davies, Donald M. McDonald, Peter Baluk, and Broniek Pytowski for criticism and suggestions for the manuscript; and Drs. Klaus Pfeffer (University of Dusseldorf, Dusseldorf, Germany) and Jonathon Sedgwick (Eli Lilly, Indianapolis, IN) for providing us with the LT β R and LT α mutant mice, respectively. This work was supported by National Institutes of Health Grant DK067989-01 (to S.A.L.) and Department of Defense Grant BC044819 (to M.S.).

- Oliver G, Alitalo K (2005) *Annu Rev Cell Dev Biol* 21:457–483.
- Alitalo K, Tammela T, Petrova TV (2005) *Nature* 438:946–953.
- Palfreman RT, Jung S, Cheng G, Weninger W, Luo Y, Dorf M, Littman DR, Rollins BJ, Zweierink H, Rot A, von Andrian UH (2001) *J Exp Med* 194:1361–1373.
- Randolph GJ, Angeli V, Swartz MA (2005) *Nat Rev Immunol* 5:617–628.
- Cassella M, Skobe M (2002) *Ann NY Acad Sci* 979:120–130.
- Pepper MS, Tille JC, Nisato R, Skobe M (2003) *Cell Tissue Res* 314:167–177.
- Kerjaschki D, Regele HM, Moosberger I, Nagy-Bojarski K, Watschinger B, Soleiman A, Birner P, Krieger S, Hovorka A, Silberhumer G, et al. (2004) *J Am Soc Nephrol* 15:603–612.
- Maruyama K, Ii M, Cursiefen C, Jackson DG, Keino H, Tomita M, Van Rooijen N, Takenaka H, D'Amore PA, Stein-Streilein J, et al. (2005) *J Clin Invest* 115:2363–2372.
- Baluk P, Tammela T, Ator E, Lyubynska N, Achen MG, Hicklin DJ, Jeltsch M, Petrova TV, Pytowski B, Stacker SA, et al. (2005) *J Clin Invest* 115:247–257.
- Kaiserling E (2001) *Lymphology* 34:22–29.
- Middel P, Raddatz D, Gunawan B, Haller F, Radzun HJ (2006) *Gut* 55:220–227.
- Paavonen K, Mandelin J, Partanen T, Jussila L, Li TF, Ristimaki A, Alitalo K, Konttinen YT (2002) *J Rheumatol* 29:39–45.
- Kerjaschki D, Huttary N, Raab I, Regele H, Bojarski-Nagy K, Bartel G, Krober SM, Greinix H, Rosenmaier A, Karhofer F, et al. (2006) *Nat Med* 12:230–234.
- Kerjaschki D (2005) *J Clin Invest* 115:2316–2319.
- Angeli V, Ginhoux F, Llodra J, Quemeneur L, Frenette PS, Skobe M, Jessberger R, Merad M, Randolph GJ (2006) *Immunity* 24:203–215.
- Takemura S, Braun A, Crowson C, Kurtin PJ, Cofield RH, O'Fallon WM, Goronzy JJ, Weyand CM (2001) *J Immunol* 167:1072–1080.
- Amft N, Curnow SJ, Scheel-Toellner D, Devadas A, Oates J, Crocker J, Hamburger J, Ainsworth J, Mathews J, Salmon M, et al. (2001) *Arthritis Rheum* 44:2633–2641.
- Hjelmstrom P (2001) *J Leukoc Biol* 69:331–339.
- Stassi G, De Maria R (2002) *Nat Rev Immunol* 2:195–204.
- Aloisi F, Pujol-Borrell R (2006) *Nat Rev Immunol* 6:205–217.
- Drayton DL, Liao S, Mounzer RH, Ruddle NH (2006) *Nat Immunol* 7:344–353.
- Armengol MP, Cardoso-Schmidt CB, Fernandez M, Ferrer X, Pujol-Borrell R, Juan M (2003) *J Immunol* 170:6320–6328.
- Cupeo T, Jansen W, Kraal G, Mebius RE (2004) *Immunity* 21:655–667.
- Martin AP, Coronel EC, Sano G, Chen SC, Vassileva G, Canasto-Chibuque C, Sedgwick JD, Frenette PS, Lipp M, Furtado GC, Lira SA (2004) *J Immunol* 173:4791–4798.
- Chen SC, Vassileva G, Kinsley D, Holzmann S, Manfra D, Wiekowski MT, Romani N, Lira SA (2002) *J Immunol* 168:1001–1008.
- Luther SA, Lopez T, Bai W, Hanahan D, Cyster JG (2000) *Immunity* 12:471–481.
- Pepper MS, Skobe M (2003) *J Cell Biol* 163:209–213.
- Nagy JA, Vasile E, Feng D, Sundberg C, Brown LF, Detmar MJ, Lawitts JA, Benjamin L, Tan X, Manseau EJ, et al. (2002) *J Exp Med* 196:1497–1506.
- Hong YK, Lange-Asschenfeldt B, Velasco P, Hirakawa S, Kunstfeld R, Brown LF, Bohlen P, Senger DR, Detmar M (2004) *FASEB J* 18:1111–1113.
- Roberts N, Kloos B, Cassella M, Podgrabinska S, Persaud K, Wu Y, Pytowski B, Skobe M (2006) *Cancer Res* 66:2650–2657.
- Al-Rawi MA, Mansel RE, Jiang WG (2005) *Eur J Surg Oncol* 31:117–121.
- Weetman AP, McGregor AM (1994) *Endocr Rev* 15:788–830.
- Breiteneder-Geleff S, Soleiman A, Kowalski H, Horvat R, Amann G, Kriehuber E, Diem K, Weninger W, Tschachler E, Alitalo K, Kerjaschki D (1999) *Am J Pathol* 154:385–394.
- Wigle JT, Oliver G (1999) *Cell* 98:769–778.
- Jackson DG (2004) *Acta Pathol Microbiol Immunol Scand* 112:526–538.
- Podgrabinska S, Braun P, Velasco P, Kloos B, Pepper MS, Skobe M (2002) *Proc Natl Acad Sci USA* 99:16069–16074.
- Wigle JT, Harvey N, Detmar M, Lagutina I, Grosfeld G, Gunn MD, Jackson DG, Oliver G (2002) *EMBO J* 21:1505–1513.
- Marinkovic T, Garin A, Yokota Y, Fu YX, Ruddle NH, Furtado GC, Lira SA (2006) *J Clin Invest* 116:2622–2632.
- Bjorndahl M, Cao R, Nissen LJ, Clasper S, Johnson LA, Xue Y, Zhou Z, Jackson D, Hansen AJ, Cao Y (2005) *Proc Natl Acad Sci USA* 102:15593–15598.
- Futterer A, Mink K, Luz A, Kosco-Vilbois MH, Pfeffer K (1998) *Immunity* 9:59–70.
- Browning JL, Allaire N, Ngam-Ek A, Notidis E, Hunt J, Perrin S, Fava RA (2005) *Immunity* 23:539–550.
- Drayton DL, Chan K, Lesslauer W, Lee J, Ying XY, Ruddle NH (2002) *Adv Exp Med Biol* 512:43–48.
- Drayton DL, Ying X, Lee J, Lesslauer W, Ruddle NH (2003) *J Exp Med* 197:1153–1163.
- Korner H, Cook M, Riminton DS, Lemckert FA, Hoek RM, Ledermann B, Kontgen F, Fazekas de St Groth B, Sedgwick JD (1997) *Eur J Immunol* 27:2600–2609.
- Ware CF (2005) *Annu Rev Immunol* 23:787–819.
- Salven P, Mustjoki S, Alitalo R, Alitalo K, Raffii S (2003) *Blood* 101:168–172.
- Liao S, Ruddle NH (2006) *J Immunol* 177:3369–3379.
- Dejardin E, Droin NM, Delhase M, Haas E, Cao Y, Makris C, Li ZW, Karin M, Ware CF, Green DR (2002) *Immunity* 17:525–535.
- Drayton DL, Bonizzi G, Ying X, Liao S, Karin M, Ruddle NH (2004) *J Immunol* 173:6161–6168.
- Shinkai Y, Rathbun G, Lam KP, Oltz EM, Stewart V, Mendelsohn M, Charron J, Datta M, Young F, Stall AM, et al. (1992) *Cell* 68, 855–67.